**NURETH14-209** 

# CFD MODELING OF SODIUM SPRAY COMBUSTION

Pratap Sathiah, Arné Siccama and Ferry Roelofs Nuclear Research and Consultancy Group (NRG), Westerduinweg 3, 1755ZG, Petten, The Netherlands

#### **Abstract**

A sodium cooled fast reactor is one of the attractive concept for the  $IV^{th}$  generation advanced reactor designs. For the safety of a sodium cooled fast reactor, sodium-air and sodium-water reactions must be avoided. A sodium-air reaction typically occurs in two dominant modes, namely the spray fire and pool fire. The focus of the paper will be on spray fires. To avoid sodium-air accidents and to mitigate the consequences if a sodium fire occurs, it is essential to understand all the physical phenomena involved in sodium spray combustion. Numerical modeling is one of the methods, which can be used to understand all the physics involved. The goal of the work presented in this paper is to propose a numerical method to simulate sodium spray combustion and to validate this method against experiments. Free falling single droplet sodium spray combustion experiments are used as a validation case for the proposed numerical method. The trend obtained using our numerical simulations matches well with the experimental data. Further validation needs to be performed, before the presented modeling can be used for sodium fast reactor safety analyses.

## 1 Introduction

A sodium cooled fast reactor is under consideration as  $IV^{th}$  generation advanced fast neutron nuclear reactor. The sodium cooled reactor concept has a reasonable experience base and large scale reactors have been built and are in operation worldwide. Liquid sodium is used as a coolant, since it has excellent thermophysical properties. In particular, it has a high thermal conductivity, a low absorption rate of fast neutrons and a possibility for breeding and plutonium and minor actinide burning good fuel breeding performance. Moreover, it can be present in liquid state across a wide range of temperatures.

However, liquid sodium has a serious shortcoming. Sodium when exposed to air or water reacts violently, which can be a potential fire hazard in a nuclear reactor. A sodium leak, which may result from a pipe break up, releases into the containment in the form of spray or jet. A part of the released sodium gets collected at the floor and may form a sodium pool. Leaked sodium essentially burns in two different modes i.e., spray and pool modes. The spray mode of burning is more severe than the pool mode of burning, since a sodium spray burns at a higher rate (burns in highly divided state i.e., in the form of the droplets). Furthermore, sodium spray fires are less easy to extinguish in comparison to sodium pool fires. However, pool combustion

continues for a longer time in comparison to spray combustion. During a sodium spray or pool combustion, sodium reacts with air and water to form several sodium by-products e.g., sodium oxide (Na<sub>2</sub>O), sodium dioxide (Na<sub>2</sub>O<sub>2</sub>) and sodium hydroxide (NaOH), which releases in the atmosphere in the form of aerosols. These aerosols are particles with a diameter ranging from  $0.1\mu m$  to  $10\mu m$ , which can cause structural damage to equipments and to public health.

In the past, several reactor accidents were reported in literature [1, 2]. In the United Kingdom (UK), a major sodium leak was reported in 1960 in steam generator of Prototype Fast Reactor (PFR). In the United States (US), a sodium fire occurred in May 1970 in a 94 megawatt-electric (MWe) sodium cooled fast reactor (Fermi 1). In the year 1995, the Japanese SFR Monju was shut down after a sodium leakage accident. The sodium leak from the secondary circuit occurred in a piping room of the reactor auxiliary building. The large scale French fast neutron reactor, Superphenix was shut down in 1997 as a result of sodium leaks in the reactor vessel. In Russia, several accidents in sodium cooled fast reactor occurred in BR-5/10, BOR-60 (experimental reactors), BN-350 (prototype reactor) and BN-600 (demonstration reactor). To summarize, sodium leakages, which lead to sodium reactions are dangerous for the safety of reactor. For the safety of sodium cooled reactor, sodium reactions must be avoided and the consequence should be mitigated. Hence, detailed experimental and numerical investigation of sodium reactions is important. Understanding sodium reactions with air and water is essential to develop computer codes, which can be used for the safety analyses of such reactors.

In the last 40 years, several research works have been performed to numerically and experimentally investigate sodium spray combustion and there is a considerable amount of literature on sodium spray combustion. In 1979, Tsai [3] developed the NACOM code for the analysis of sodium spray fires in SFRs. The vapor-phase combustion theory [4] was used to model the burning of a single droplet. A computer program SOFIA-II was developed by Kawabe et al. [5] to predict pressure and temperature transients of their own measurements. The calculated pressure was in agreement with experiments. Malet et al. [6] developed the PULSAR code to predict a sodium spray fire. The code was validated against their own experiments. The SPHINCS [7, 8] code developed by Japan Nuclear Cycle Development Institute (JNCDI) is used for safety evaluation of sodium cooled fast reactors. This code uses a spray model developed by Tsai [3]. AQUA-SF was developed by Takata et al. [2, 7, 9] which simulates burning of sodium in both the spray and pool modes. The code was validated against experiments of Ohno et al. [10] and Nagai et al. [11].

The COMET code, developed by JNCDI is used for Direct Numerical Simulation (DNS) of combustion of a free falling single sodium droplet by Okano and Yamaguchi [12]. The flow was solved with the unsteady Navier-Stokes equations and chemistry was assumed to be in equilibrium. They simulated a free falling single droplet sodium experiment of Miyahara and Ara. SOMIX is another widely used code developed by Heisler and Mori [13] in 1977. SOMIX-1 uses vapor-phase combustion model, while SOMIX-2 adopted Krolikowski's [14] diffusion model for the calculation of burning rate of sodium in air. Both versions of the code had problems in predicting spray fires with high oxygen concentration.

In this article, we report a Computational Fluid Dynamics (CFD) modeling study of sodium spray combustion. In particular, it presents validation of CFD based sodium spray combustion solver against free falling single droplet experiment. The article is organized as follows. In section 2, numerical methodology is presented. Governing equations for continuous and lagrangian phase are described here. The spray evaporation models are also described here. Section 3 presents the description of the experiment and validation results. Finally, the conclusion is presented in section 4.

## 2 Numerical methods

Commercial CFD ANSYS FLUENT [15] solver and Favre-Averaged Navier-Stokes (FANS) approach are used for this purpose. The gaseous phase was simulated in Eulerian phase, while spray droplets were tracked in Lagrangian phase. The models and the governing equations are described below in following subsections.

## 2.1 Eulerian phase governing equations

Within ANSYS FLUENT[15] solves the following governing equation for conservation of mass, momentum, energy and mixture fraction. These equations are given as follows Mass:

$$\frac{\partial \bar{\rho}}{\partial t} + \frac{\partial}{\partial x_j} (\bar{\rho} \tilde{u}_i) = S_m. \tag{1}$$

Velocity:

$$\frac{\partial}{\partial t}(\bar{\rho}\tilde{u}_i) + \frac{\partial}{\partial x_j}(\bar{\rho}\tilde{u}_i\tilde{u}_j) = -\frac{\partial\bar{p}}{\partial x_j} + \frac{\partial}{\partial x_j}(\bar{\tau}_{ij} - \bar{\rho}\widetilde{u_i''u_j''}) + g_i\frac{\tilde{u}_i}{\bar{\rho}}S_m. \tag{2}$$

Mixture fraction (fuel mass fraction):

$$\frac{\partial}{\partial t}(\bar{\rho}\tilde{f}) + \frac{\partial}{\partial x_i}(\bar{\rho}\tilde{u}_i\tilde{f}) = \frac{\partial}{\partial x_i}\left(\frac{\mu_t}{\sigma_t}\frac{\partial\tilde{f}}{\partial x_i}\right) + S_m \tag{3}$$

Variance of mixture fraction:

$$\frac{\partial}{\partial t}(\bar{\rho}\widetilde{f'^2}) + \frac{\partial}{\partial x_j}(\bar{\rho}\widetilde{u}_i\widetilde{f'^2}) = \frac{\partial}{\partial x_j}\left(\frac{\mu_t}{\sigma_t}\frac{\partial\widetilde{f'^2}}{\partial x_j}\right) + C_g\mu_t\left(\frac{\partial\widetilde{f}}{\partial x_j}\right)^2 - C_d\bar{\rho}\frac{\epsilon}{k}\widetilde{f'^2}$$
(4)

Energy conservation equation:

$$\frac{\partial}{\partial t}(\bar{\rho}\tilde{H}) + \frac{\partial}{\partial x_j}(\bar{\rho}\tilde{u}_i\tilde{H}) = \frac{\partial}{\partial x_j}\left(\frac{k_t}{C_p}\frac{\partial\tilde{H}}{\partial x_j}\right) + S_h. \tag{5}$$

Here,  $\tilde{u_i}$ ,  $\tilde{f}$  and  $\tilde{H}$  are the Favre-averaged (density-weighted) velocity, mixture fraction and total enthalpy,  $\mu_t$  is the turbulent viscosity,  $\sigma_t$  is the turbulent Schmidt number,  $k_t$  is the thermal conductivity and  $S_m$  is the mass transfer to the gas phase from liquid droplet due to evaporation. t is the time,  $\rho$  is the density, p is the pressure,  $C_p$  is the specific heat capacity,  $g_i$  is the gravitation acceleration. In Eq. 4  $f'=f-\tilde{f}$  is the standard deviation of mixture fraction. The default values for the constants  $\sigma_t$ ,  $C_g$ , and  $C_d$  are 0.85, 2.86, and 2.0 respectively.  $\bar{f}$  and  $\bar{f}$  are the Reynolds averaged and Favre-averaged quantities. The term  $u_i''u_j''$  in Eq. 2, is the Reynolds stress which needs to be closed. The closure for this term is described below.

# 2.2 Turbulence modeling

The closure for Reynolds stress terms in Eq. 2 was achieved with the standard  $k-\omega$  turbulence model. Following equations for turbulent kinetic energy, k and specific dissipation rate,  $\omega$  is solved:

$$\frac{\partial \bar{\rho}k}{\partial t} + \frac{\partial}{\partial x_j} (\bar{\rho}\tilde{u}_i k) = \frac{\partial}{\partial x_j} \left( \mu + \frac{\mu_t}{\sigma_k} \frac{\partial k}{\partial x_j} \right) + G_k + \underline{G_b} + \bar{\rho}\beta^* f_{\beta^*} \omega k \tag{6}$$

The 14<sup>th</sup> International Topical Meeting on Nuclear Reactor Thermal Hydraulics NURETH-14 Toronto, Ontario, Canada, September 25-30, 2011

and

$$\frac{\partial \bar{\rho}\omega}{\partial t} + \frac{\partial}{\partial x_i}(\bar{\rho}\tilde{u}_i\omega) = \frac{\partial}{\partial x_i}\left(\mu + \frac{\mu_t}{\sigma_\omega}\frac{\partial\omega}{\partial x_i}\right) + \alpha\frac{\omega}{k}G_k + \bar{\rho}\beta f_\beta\omega^2. \tag{7}$$

The turbulent viscosity  $\mu_t$  is evaluated as follows

$$\mu_t = \alpha^* \frac{\bar{\rho}k}{\omega}.\tag{8}$$

Here,  $\beta$ ,  $\beta^*$ ,  $\alpha^*$ ,  $f_{\beta}$  and  $f_{\beta^*}$  are the constants. The production term in Eq. 6 and 7 is given by

$$G_k = \left[ \mu_t \left( \frac{\partial \tilde{u}_i}{\partial x_j} + \frac{\partial \tilde{u}_j}{\partial x_i} - \frac{2}{3} \frac{\partial \tilde{u}_k}{\partial x_k} \delta_{ij} \right) - \frac{2}{3} \bar{\rho} k \delta_{ij} \right] \frac{\partial \tilde{u}_i}{\partial x_j}. \tag{9}$$

Buoyancy effects of the turbulent kinetic energy given by underlined term in Eq. 6 is taken into account and is implemented in ANSYS FLUENT using User Defined Functions (UDF). The term  $G_b$  in Eq. 6 is given as follows

$$G_b = \beta g_i \frac{\mu_t}{Pr_t} \nabla \tilde{T}. \tag{10}$$

Here,  $g_i$  is the gravitational acceleration,  $Pr_t$  is the turbulent Prandtl number and  $\beta$  is the coefficient of thermal expansion and is given by

$$\beta = -\frac{1}{\bar{\rho}} \left( \frac{\partial \bar{\rho}}{\partial T} \right)_{p}. \tag{11}$$

However, the effect of buoyancy on specific dissipation rate is not taken into account.

#### 2.3 Combustion model

It is worth reminding that we restrict our study only to sodium-air reactions. Sodium-air reaction produces sodium oxide and peroxide aerosols, which can influence radiation thereby affecting gas temperature. Since the saturation vapor pressures of the products are low, they do not exist in gas phase and must be treated as aerosols

It is often assumed in sodium combustion that chemical reactions are faster than fluid flow and chemical species diffusion. Hence, it can be simulated using chemical equilibrium approach, which means that chemical reactions are in equilibrium as soon as sodium mixes with air. The mixture fraction based combustion model is used for sodium spray combustion. In this approach, Probability Distribution Function (PDF) within a computational cell is obtained from mean mixture fraction  $\tilde{f}$  and variance of mixture fraction  $\tilde{f}^{\prime 2}$ , which is obtained from solution of Eq. 3 and 4. The PDF is assumed to be of Beta-PDF type [16]. The Favre-averaged mean value of temperature and species mass fraction in a cell is obtained by the following equation.

$$\tilde{T} = \int_0^1 T(f, H) P(f, f') df \tag{12}$$

and

$$\tilde{Y}_k = \int_0^1 Y_k(f, H) P(f, f') df. \tag{13}$$

In the above equation, T(f) and  $Y_k(f)$  are obtained from non-adiabatic equilibrium PDF table. Equilibrium calculations were performed for sodium-air system at 298 K and 1 atm using ANSYS FLUENT. Following gas phase species N, NO, NO<sub>2</sub>, NO<sub>3</sub>, N<sub>2</sub>O, N<sub>2</sub>O<sub>3</sub>, N<sub>2</sub>O<sub>4</sub>,

N<sub>2</sub>O<sub>5</sub>, N<sub>3</sub>, Na, NaNO<sub>2</sub>, NaNO<sub>3</sub>, NaO, Na<sub>2</sub>, Na<sub>2</sub>O, Na<sub>2</sub>O<sub>2</sub>, O, O<sub>2</sub> and O<sub>3</sub> and condensed phase species Na(cr), Na(l), NaO<sub>2</sub>(cr), NaO<sub>2</sub>(l), Na<sub>2</sub>O(c), Na<sub>2</sub>O(b), Na<sub>2</sub>O(a), Na<sub>2</sub>O(l), Na<sub>2</sub>O<sub>2</sub>(b), Na<sub>2</sub>O<sub>2</sub>(a), Na<sub>2</sub>O<sub>2</sub>(l), NaNO<sub>2</sub>(a), NaNO<sub>2</sub>(b), NaNO<sub>2</sub>(l), NaNO<sub>3</sub>(a) NaNO<sub>3</sub>(b) and NaNO<sub>3</sub>(l) are considered for the equilibrium calculation. The letters in parentheses for condensed phase species indicates their physical form: l = liquid; cr = crystalline; a, b, and c = various solid forms. In order to compare results obtained from ANSYS FLUENT, separate calculations were performed using NASA CEA code [17]. The code is written by Gordon and Mcbride [18] which calculates the adiabatic flame temperature and equilibrium composition by using the Gibb's free energy minimization [19] procedure based on the element potential method. The results obtained using this code is compared with ANSYS FLUENT. Fig 1 and 2 shows comparison of temperature, mass fraction of Na, Na<sub>2</sub>O and Na<sub>2</sub>O<sub>2</sub> versus mixture fraction. The curves with crosses and circles show ANSYS FLUENT and NASA CEA results respectively. Similarity of the results between these codes verifies that ANSYS FLUENT results are accurate.

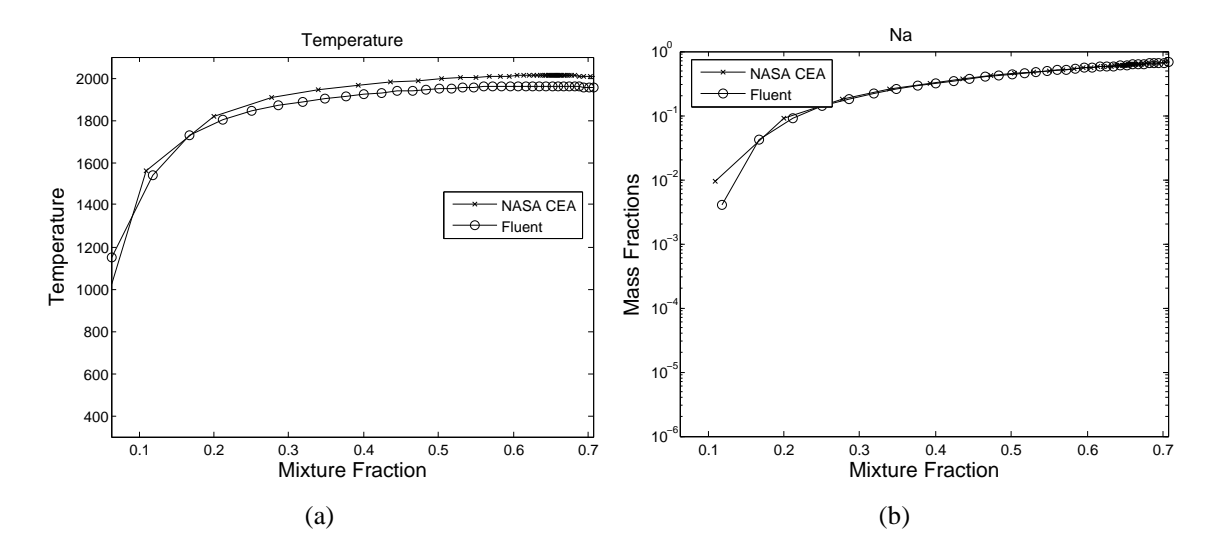


Figure 1: a) Temperature versus mixture fraction b) Mass fractions of Na versus mixture fraction

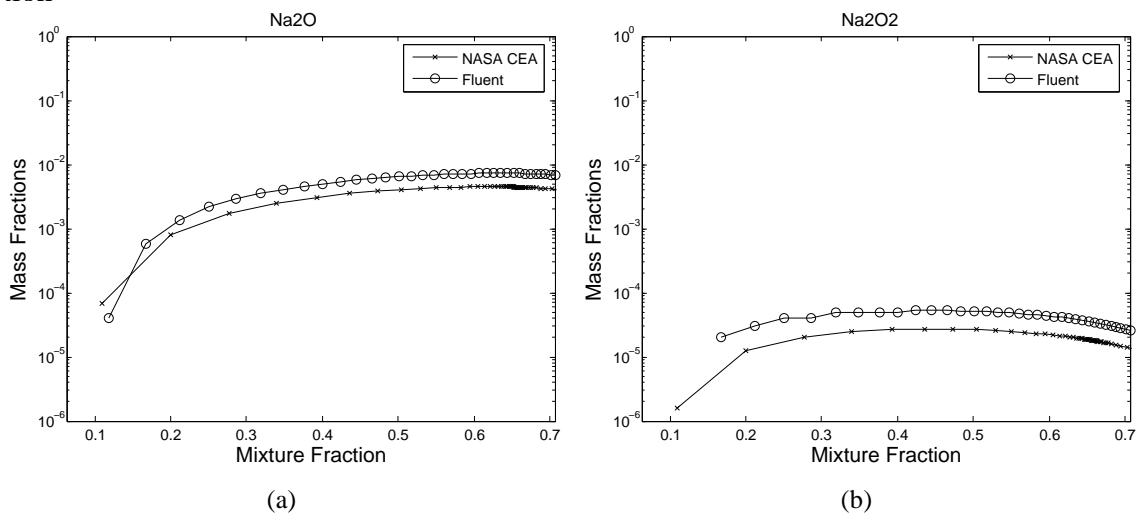


Figure 2: a) Mass fraction of Na<sub>2</sub>O versus mixture fraction b) Mass fraction of Na<sub>2</sub>O<sub>2</sub> versus mixture fraction

### 2.4 Lagrangian phase equations

The spray droplets were assumed as discrete particles. These droplets were tracked in Lagrangian phase in ANSYS FLUENT. The particle motion was obtained by integrating the force balance on particle. The integration leads to the following equation:

$$\frac{du_p}{dt} = F_D(u - u_p) + \frac{g_i(\rho - \rho_g)}{\rho_p} + F_x \tag{14}$$

for the velocity of the particle. Here,  $F_x$  is the additional acceleration per unit mass, the term  $F_D(u-u_p)$  is the drag force per unit particle mass. Here,  $F_D$  is given as follows:

$$F_D = \frac{18\mu}{\rho D^2} \frac{C_d Re}{24}$$
 (15)

where,  $C_d$  is the drag coefficient for sodium [3] and is given as follows

$$C_d = \begin{cases} 24/Re & \text{if } Re < 0.1\\ 2.6 + 23.71/Re & \text{if } 0.1 < Re < 6\\ 18.5/Re^{0.6} & \text{if } 6 < Re < 500\\ 4/9 & \text{if } Re > 500 \end{cases}$$

$$(16)$$

Re is the Reynolds number which is given by

$$Re = \frac{\rho D|u_p - u|}{\mu} \tag{17}$$

where  $\rho$  is the density of particle, u is the gas velocity, D is the diameter of the particle. The particle position was obtained by integrating the following equation

$$\frac{dx}{dt} = u_p \tag{18}$$

where x is the position of the particle and  $u_p$  is the velocity of the particle.

Turbulent dispersion of the particles was accounted by stochastic tracking method. In this approach, affect of instantaneous velocity on the particle velocity was taken into account by using a stochastic method. The details of the model are described in [15].

The liquid sodium droplets undergo evaporation and evaporated sodium when comes in contact with air starts reacting. To track the evaporation of the particle, equation for the mass and temperature of the particle must be solved which are given below.

$$\frac{dm_d}{dt} = \dot{m_d} \tag{19}$$

and

$$m_d C_p \frac{dT_p}{dt} = h A_p (T_\infty - T_p) + \frac{dm_d}{dt} h_{fg} + \epsilon_p A_p \sigma(\theta^4 - T_p^4). \tag{20}$$

Here,  $m_d$  is the mass of particle,  $\dot{m_d}$  is the mass burning rate of droplet,  $C_p$  is the specific heat of particle at constant pressure,  $A_P$  is the area of particle,  $T_\infty$  is the local temperature of continuous phase, h is the heat transfer coefficient,  $\epsilon_p$  is the particle emissivity and  $\sigma$  is the Stefan's Boltzmann constant. Equation 20 models heat exchange between particle and continuous phase through convection, latent heat transfer and radiation, described by first, second and third term respectively. The model for mass burning rate of droplet,  $\dot{m_d}$  is described in the next subsection.

#### 2.4.1 Spray evaporation model

Recently, the model proposed by Tsai [3] is used by Takata et al. [9] to simulate sodium spray combustion. Tsai suggested that the combustion of sodium droplet is divided into two stages a) pre-ignition and b) post-ignition. For sodium combustion, pre-ignition is important and must be accounted in modelling of sodium combustion. In the pre-ignition stage, a film of oxide is formed on droplet surface by surface oxidation. Heat produced by oxidation is fed back to droplet surface, thereby increasing droplet temperature. The droplet ignition starts when droplet ignition temperature is reached. Existence of pre-ignition phase is also confirmed experimentally by Yuasa [20]. A detailed description of pre-ignition and post-ignition model is presented below.

#### **Pre-ignition model**

In the pre-ignition model, it was assumed that 1) the oxide film is very thin and does not stop diffusion of oxygen to the droplet surface 2) the change of droplet diameter is negligible 3) heat transfer from sodium to gas can be neglected, because of high thermal conductivity of sodium 4) zero oxygen concentration at droplet surface and 5) no viscous force.

The mass flux,  $\dot{m}$ , of fuel evapourating from the droplet is given by

$$\dot{m} = N_o A_p M w_{O_2}. \tag{21}$$

Here,  $N_o$  is the molar flux of oxygen into the sodium surface,  $A_p$  is the area of the droplet and  $Mw_{O_2}$  is the molecular weight of fuel species. The molar flux of oxygen can be evaluated as follows:

$$N_o = k_c \frac{(C_{o,\infty} - C_{o,s})}{r} \tag{22}$$

where,  $k_c$  is the mass transfer coefficient,  $C_{o,s}$  and  $C_{o,\infty}$  are the concentration of oxygen on the droplet surface and in the surroundings. The mass transfer coefficient,  $k_c$  is evaluated using Ranz-Marshall correlation [21] for free falling droplet:

$$Sh = \frac{k_c D}{D_d} = (2 + 2C_1 Re^{1/2} Sc^{1/3})$$
(23)

where constant  $C_1$ =0.3, Sc is the Schmidt number. The correlation taken into account effects of forced convection on the mass burning rate which increases due to change in the shape of the droplet. After rearranging, mass burning rate of fuel droplet is given by

$$\dot{m} = \pi \rho_g M w_{O_2} D_d D S h \frac{Y_{O_2, \infty} - Y_{O_2, s}}{r} = \frac{\pi C D_d Y_{O_2} D}{r} S h.$$
 (24)

Here,  $\dot{m_d}$  is the mass burning rate of falling droplet, C is the molar density,  $D_d$  is the diffusion coefficient,  $Y_{O_2,\infty}$  is the oxygen mole fractions in ambient,  $Y_{O_2,\infty}$  is the oxygen mole fractions on the droplet surface and r is the stoichiometric ratio. The particle temperature is obtained by solving Eq. 20. Since there is no evaporation during the pre-ignition phase, second term in Eq. 20 (i.e.,  $h_{fg}$ ) is replaced by  $h_{reac}$ . Here,  $h_{reac}$  is the amount of heat generated during the surface reaction of sodium in J/kg. During the surface reaction, sodium reacts with oxygen to form Na<sub>2</sub>O<sub>2</sub> and Na<sub>2</sub>O. In addition, it is assumed that 0.26 moles of sodium forms Na<sub>2</sub>O<sub>2</sub> and 0.74 forms Na<sub>2</sub>O, the heat of reaction is accordingly calculated as done by Karthikeyan et al. [22].

#### Post-ignition model

Once the droplet ignites, it moves into post-ignition stage. The mass burning rate in this case is obtained from vapor phase combustion theory ( $D^2$ -law) of Spalding [4] as suggested by Tsai. This theory is well established for spray combustion of hydrocarbons. However, it can also be applied for sodium combustion, since sodium droplet also follows  $D^2$ -law. In vapor-phase combustion theory, it is assumed that a spherical burning flame or zone was surrounded by stationary droplet. The evaporated fuel, when reaches the burning zone, is consumed by the flame instantaneously under steady state conditions. Under this assumption, it can be postulated that burning rate of fuel is controlled by evaporation of fuel, which in turn is controlled by the heat transfer to droplet. Here, the mass burning rate is given by

$$\dot{m} = \frac{\pi \rho DK}{4}.\tag{25}$$

Here, K is the burning rate coefficient [2, 4, 9] or evaporation constant and is given by

$$K = \frac{8k_g}{C_p \rho} ln(1+B) \tag{26}$$

where  $k_g$  is the gas mixture thermal conductivity,  $C_p$  is the gas mixture specific heat capacity, and B is the transfer number. The transfer number is defined as

$$B = \frac{1}{h_{fg}} \left( C_p(T_g - T_s) + \frac{H_c Y}{r} \right). \tag{27}$$

Here,  $T_g$ ,  $T_s$  are the gas and the surface temperature,  $h_{fg}$  is the latent heat of evaporation and  $H_c$  is the heat of combustion, Y is the mole fraction of oxygen. The mass burning rate of a single droplet is obtained as follows

$$\dot{m}_d = \dot{m}Nu = \frac{2\pi k}{C_p}DNu[ln(1+B)].$$
 (28)

Here, Nusselt number, Nu in Eq. 28 is obtained from Ranz and Marshall [21] correlation as follows

$$Nu = (2 + 2C_1 Re^{1/2} Pr^{1/3}). (29)$$

where, Pr is the Prandtl number. The particle temperature is obtained by solving Eq. 20. The spray burning rate is the summation of burning rates of individual droplets.

For spray size distribution the Nukiyama-Tanasawa [23] correlation is used here, which is expressed as follows

$$\frac{dR_v}{dD} = \left(\frac{3.915}{\bar{D}}\right)^6 \frac{D^5}{120} exp\left(-\frac{3.915D}{\bar{D}}\right). \tag{30}$$

Here,  $\bar{D}$  is the volume mean diameter and  $R_v$  is the volume fraction of spray which contains droplet of diameters smaller than D. This size distribution is used in order to calculate the surface mean drop diameter from the volume mean drop diameter.

To summarize, at every flow time step Eq. 1, 2, 3, 4 and 5 are solved to obtain velocity, pressure mixture fraction, variance of mixture fraction and temperature. At every particle time step Eq. 14, 18, 19 and 20 are solved to obtain velocity, position, mass and temperature of the particle. The mass loss rate in Eq. 19 can be obtained either by pre-ignition model i.e, Eq. 24 or postignition model i.e., Eq. 28. The pre-ignition model is invoked when the droplet temperature is

lower than ignition temperature,  $T_{ign}$ . Above this temperature, gas phase reaction is important and hence post-ignition model is used. In our simulations, ignition temperature of 873 K is assumed, this value is also recommended by Takata et al. [9]. At each time step particle mass source, mixture fraction source and energy source terms are updated. The Reynolds number, Schmidt number and Prandtl numbers used for particle properties calculation are evaluated at film temperature using Sparrows  $1/3^{rd}$  rule as follows

$$T_{film} = \frac{2T_p + T_b}{3}. (31)$$

where,  $T_p$  and  $T_b$  are the particle temperature and bulk temperature.

#### 2.5 Numerical scheme

3D simulations were performed using ANSYS FLUENT, which employs a finite volume method. The spatial and time discretization of the conservation equations are performed with second order upwind scheme and second-order implicit method, respectively. The pressure-velocity coupling is performed with SIMPLE and discretized equations were solved using a segregated solver in an iterative manner. The particle trajectories are obtained by integrating the equation of force balance, which is achieved by using a  $5^{th}$  order Runge-Kutta scheme [24].

UDF in ANSYS FLUENT is used to implement temperature dependent sodium properties (e.g., diffusivity, enthalpy of vaporization and vapor pressure), drag laws and spray evaporation models. The particle source terms for mass, mixture fraction and energy ( $S_m$  and  $S_h$  in Eq. 1, 3 and 5) are also implemented using UDF.

## 3 Results and discussion

The aim of this work is to propose a numerical approach and perform validation using the proposed approach. For this purpose, free falling single sodium droplet experiments, which were conducted by Miyahara and Ara [25] in 1998 is used for the validation. A single droplet of uniform diameter 3.8 mm with a temperature of 773 K was injected into an ambient atmosphere (pressure of 1 atm and temperature of 298 K). The droplet falls from a height of 2.7 m. The burned mass and falling velocities are measured at two different locations of 0.1 m and 2.4 m. The air temperature and oxygen concentration are kept constant. The initial condition and the measurement results are reported in the Table 1 and 2, respectively.

Table 1: Initial condition of free falling droplet experiments [25].

Phase	Variable	Value
Droplet	Diameter	3.8 mm
	Temperature	775 K
Air	Temperature	290 K
	Pressure	1 atm

A three dimensional cuboidal computational domain (height of 6 m, depth and width of 1.5 m) is used to perform simulations. The boundaries of the domain are defined as walls and adiabatic boundary condition for temperature is applied. A single particle with droplet diameter of 3.8 mm and droplet temperature of 775 K is injected at location of 0.2 m from the top respectively.

Table 2: Results of free falling droplet experiment [25].

Droplet Velocity	Falling Distance at 0.1 m	$1.3 \pm 0.33 \text{ m/s}$
	Falling Distance at 2.4 m	$5.5 \pm 0.48 \text{ m/s}$
Droplet Burnt Mass	Falling Distance at 2.7 m	$3.37 \pm 0.69 \text{ mg}$

The simulation results are compared with the experiments. Figure 3a shows the variation of the droplet temperature with time obtained using numerical simulations. The figure clearly indicates that until time t=0.5 s, the droplet temperature increases gradually and then the droplet temperature (is equal to the boiling point of sodium) is constant. The temperature increases from initial temperature of T=775 K to T=873 K is because of pre-ignition phase (surface reaction), while the increase in temperature from T=873 K to T=1149 K is attributed to post-ignition phase (gas phase reaction).

Figure 3b shows change in droplet diameter with time during the pre-ignition and post-ignition phase. A slight increase in droplet diameter in the pre-ignition phase is because of increase in volume of the droplet due to thermal expansion. In the post-ignition phase, the droplet diameter decreases due to the combustion of the droplet.

Figure 4a and 4b shows falling distance and falling velocities versus time obtained using numerical simulations. The falling distance increases with time much faster in the beginning (t=0-0.4 s) than in the later stages. This is because of gravity force which is larger than the drag force in the beginning. However, at later stage both these forces are equal in magnitude and they counteract each other.

The falling velocities obtained using simulations are compared with experiments at falling distance of 0.1 m and 2.4 m. The falling velocities obtained are within measurement uncertainty. In Figure 5, results of droplet mass versus time obtained using numerical simulation are compared with experiments. The droplet mass decreases with time because of evaporation and combustion of droplet. The trend of droplet mass versus time matches very well with the experiments. These results are consistent with results reported in Fig. 4b.

Overall, the simulations results compares very well with this experiment, which indicate

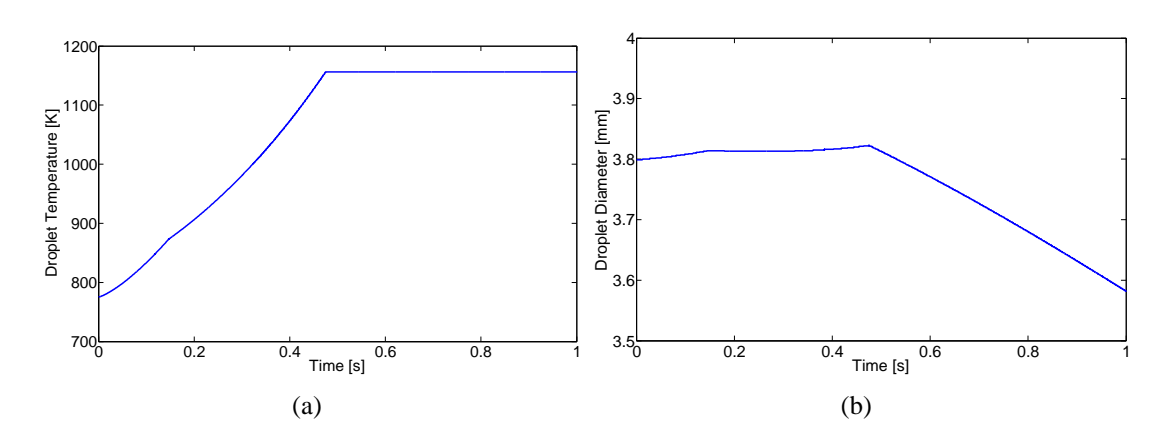


Figure 3: a) Droplet temperature  $T_p$  versus time, t. b) Droplet diameter  $d_p$  versus time, t.

that the model is able to reproduce experiments. Focus of future work will be to validate this approach against large scale multiple droplet experiments.

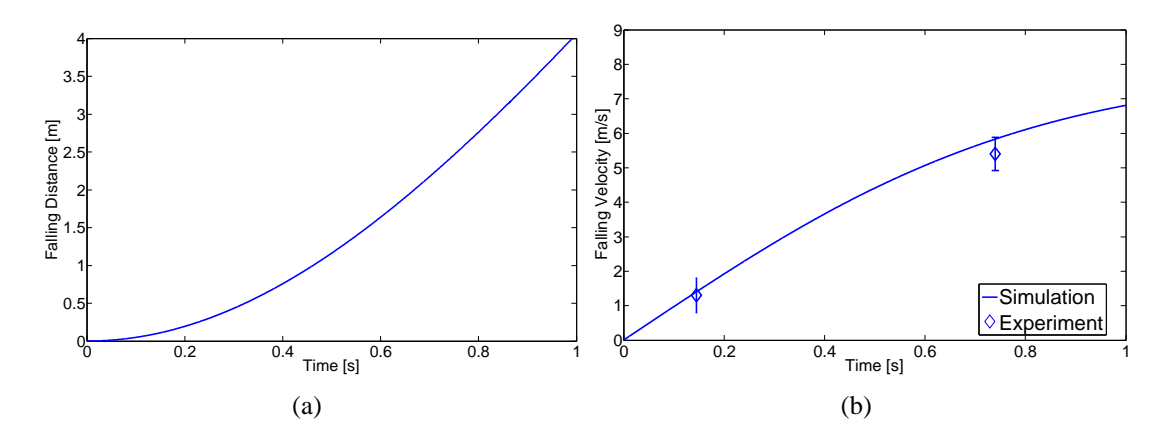


Figure 4: a) Falling distance versus time, t. b) Falling velocity versus time, t.

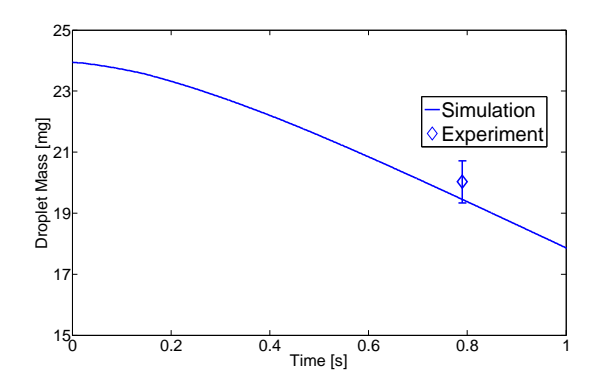


Figure 5: Droplet mass versus time, t.

# 4 Conclusion

CFD based numerical approach is proposed here to model sodium spray combustion. The model is implemented in a commercial CFD code ANSYS FLUENT using UDF. The extended code is validated against a single droplet experiments of Miyahara and Ara. The numerical results of falling velocity at 0.1 m and 2.4 m and burned mass are in good agreement with the experiments.

Further validation against large scale multiple droplet sodium experiments must be performed before this code can be used for the safety analysis of sodium fast reactors.

# 5 Acknowledgment

The work presented here was funded by the FP7 European Commission Collaborative Project ESFR No. 232658, and the Dutch Ministry of Economic Affairs. ANSYS FLUENT customer support especially Dr. Ren Liu for this work is highly appreciated.

## 6 References

[1] P. Anzieu and P. Martin. Sodium-cooled fast reactors of the future., 2011.

- [2] T. Takata. *Multi-Disciplinary Phenomena of Chemical Reaction and Thermal Hydraulics in Sodium Cooled Fast Reactor*. PhD thesis, Osaka University, 2007.
- [3] S.S. Tsai. The NACOM code for analysis of postulated sodium spray fires in LMFBRS. Technical report, Engineering and Advanced Reactor Saftey Division, Department of Nuclear Energy, Brookhaven National Laboratory, USA, 1979.
- [4] D.B. Spalding. Some Fundamentals of Combustion. Butteworths, London, England, 1955.
- [5] R. Kawabe, A. Suzuoki, and A. Minato. A study on sodium spray combustion. *Nuclear Engineering and Design*, 75:49–56, 1982.
- [6] J.S. Malet, G. Casselmann, G. D. Guy, R. Rzekiecki, and J. Charpenel. Potential results of spray and pool fires. *Nuclear Engineering and Design*, 68:195–206, 1981.
- [7] A. Yamaguchi, T. Takata, and Y. Okano. Numerical methodology to evaluate fast reactor sodium combustion. *Nuclear Technology*, 136(3):315–330, 2001.
- [8] A. Yamaguchi and Y. Tajima. Numerical simulation of non-premixed diffusion flame and reaction product aerosol behavior in liquid metal pool combustion. *Journal of Nuclear Science and Technology*, 40(2):93–103, 2003.
- [9] T. Takata, A. Yamaguchi, and I. Mackawa. Numerical investigation of multidimensional characteristics in sodium combustion. *Nuclear Engineering and Design*, 220(1):37–50, 2003.
- [10] S. Ohno. Study of sodium leak fire. PNC Techical Review, 92:19, 1994.
- [11] K. Nagai. Sodium leakage and combustion test measurement and distribution of droplet side using various spray nozzles. Technical report, 1999.
- [12] Y. Okano and A. Yamaguchi. Numerical simulation of a free-falling liquid sodium droplet combustion. *Annals of Nuclear Energy*, 30(18):1863–1878, 2003.
- [13] M.P. Heisler and K. Mori. SOMIX-1 user manual. Technical report, Rockwell International Corp., Canoga Park, CA (USA), 1977.
- [14] T.S. Krolikowski, L. Leibowitz, and R.O. Ivins. The reaction of a molten sodium spray with air in an enclosed volume part II: Theoretical model. *Nuclear Science and Engineering Mathematics*, 38:161–166, 1969.
- [15] ANSYS FLUENT. ANSYS-Fluent Inc., 2008 ANSYS-Fluent Inc., 2008. Fluent 12.0. Lebanon, N.H., 2008.
- [16] Milton Abramowitz and Irene A. Stegun, editors. *Handbook of Mathematical Functions:* with Formulas, Graphs, and Mathematical Tables (Paperback).
- [17] S. Gordon and B.J. McBride. Computer program for calculation of complex chemical equilibrium compositions and applications: Analysis. Technical report, NASA reference Publication 1311., 1994.

- [18] S. Gordon and B. J. Mcbride. Computer program for calculation of complex chemical equilibrium compositions, rocket performance, incident and reflected shocks, and chapman-jouguet detonations. Technical report, NASA Glenn Research Center, USA, 1971.
- [19] S. Turns. *An Introduction to Combustion Concepts and Applications*. McGrawhill Series in Mechanical Engineering, 2000.
- [20] S. Yuasa. Spontaneous ignition of sodium in dry and moist air streams. *Proceedings in 20th symposium on Combustion*, pages 1869–1876, 1984.
- [21] W.E. Ranz and W.R. Marshall. Evapouration from drops. *Chemical Engineering Progress*, 48:173–180, 1952.
- [22] S. Karthikeyan, T. Sundarajan, U.S.P. Shet, and P. Selvaraaj. Effects of turbulent natural convection on sodium pool combustion in the steam generator buliding of a fast breeder reactor. *Nuclear Engineering and Design*, 239(12):2992–3002, 2009.
- [23] S. Nukiyama and Y. Tanasawa. *Transactions of Society of Mechanical Engineers*, 14, 1938.
- [24] J. R. Cash and A. H. Karp. A variable order runge-kutta method for initial value problems with rapidly varying right-hand sides. *ACM Transactions on Mathematical Software*, 16:201–222, 1990.
- [25] Miyahara and Ara. Experiments of free-falling sodium droplet. Technical report, PNC TN9410 98-065, Japan Nuclear Cycle Development Institute (in Japanese), 1998.